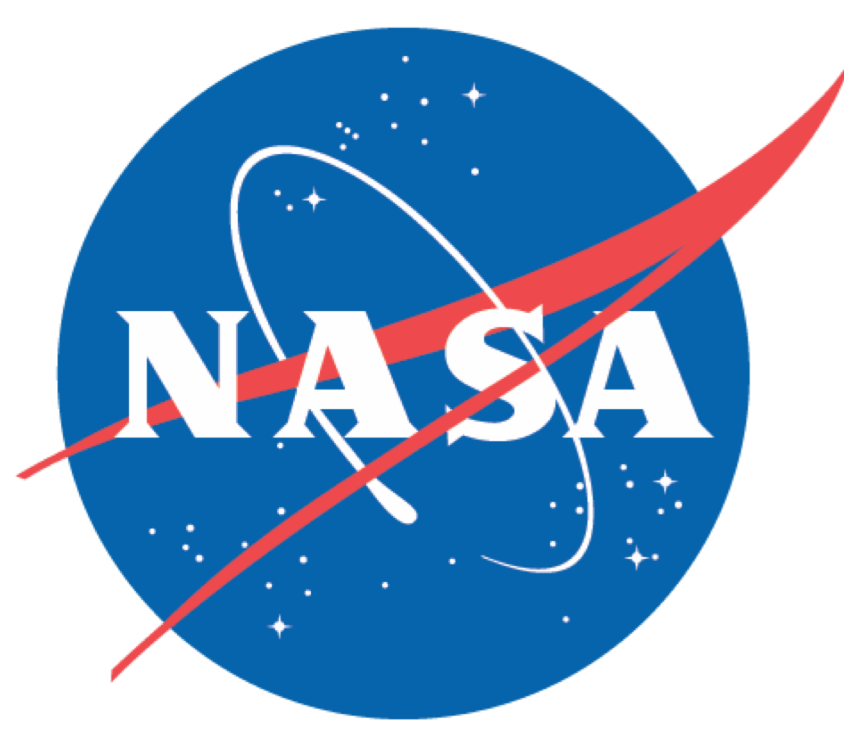


SURVEY OF SOLAR FLARE SIGNATURES IN THE UPPER IONOSPHERE WITH GNSS AND GOES OBSERVATIONS: A CASE STUDY



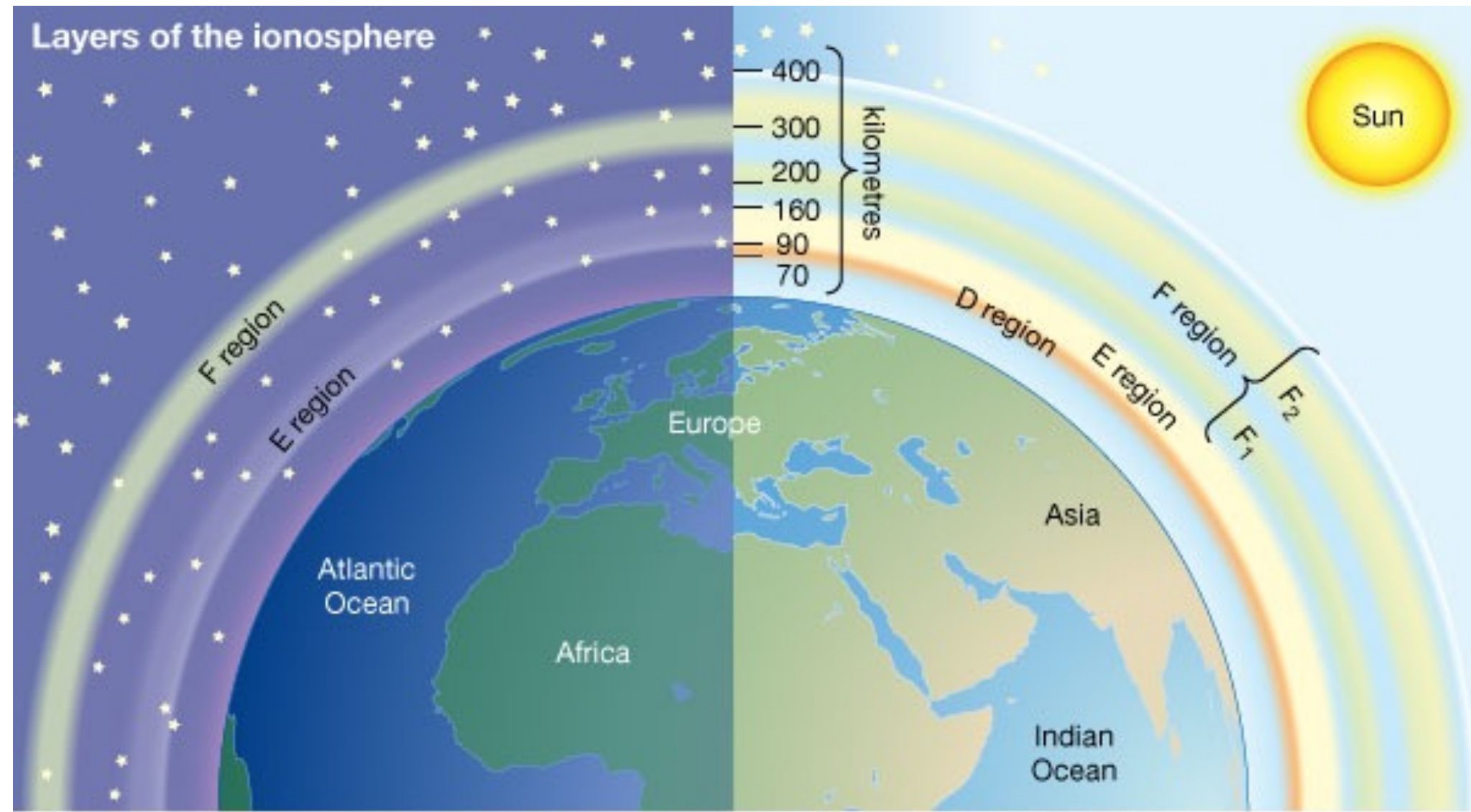
S. M. Blevins^{1,2}, L. A. Hayes³, Y. M. Collado-Vega⁴, B. P. Michael², C. E. Noll²

¹ Science Systems and Applications, Inc., Lanham, MD, USA; ² Crustal Dynamics Data Information System (CDDIS), NASA Goddard Space Flight Center, Greenbelt, MD, USA; ³ Trinity College Dublin, Ireland; ⁴ Community Coordinated Modeling Center (CCMC), NASA Goddard Space Flight Center, Greenbelt, MD, USA

Introduction

Global navigation satellite system (GNSS) phase measurements of the total electron content (TEC) and ionospheric delay are sensitive to sudden increases in electron density in the layers of the Earth's ionosphere. These sudden ionospheric disruptions, or SIDs, are due to enhanced X-ray and extreme ultraviolet radiation from a solar flare that drastically increases the electron density in localized regions. SIDs are solar flare signatures in the Earth's ionosphere and can be observed with very low frequency (~ 3-30 kHz) monitors and dual-frequency GNSS (L1 = 1575.42 MHz, L2 = 1227.60 MHz) receivers that probe lower (D-region) to upper (F-region) ionospheric layers, respectively. Figure 1 illustrates the layers in Earth's ionosphere.

Figure 1: Earth's ionosphere is ionized by radiation from the Sun; here the ionospheric layers are illustrated during both night (left) and day (right)



© 2012 Encyclopædia Britannica, Inc.

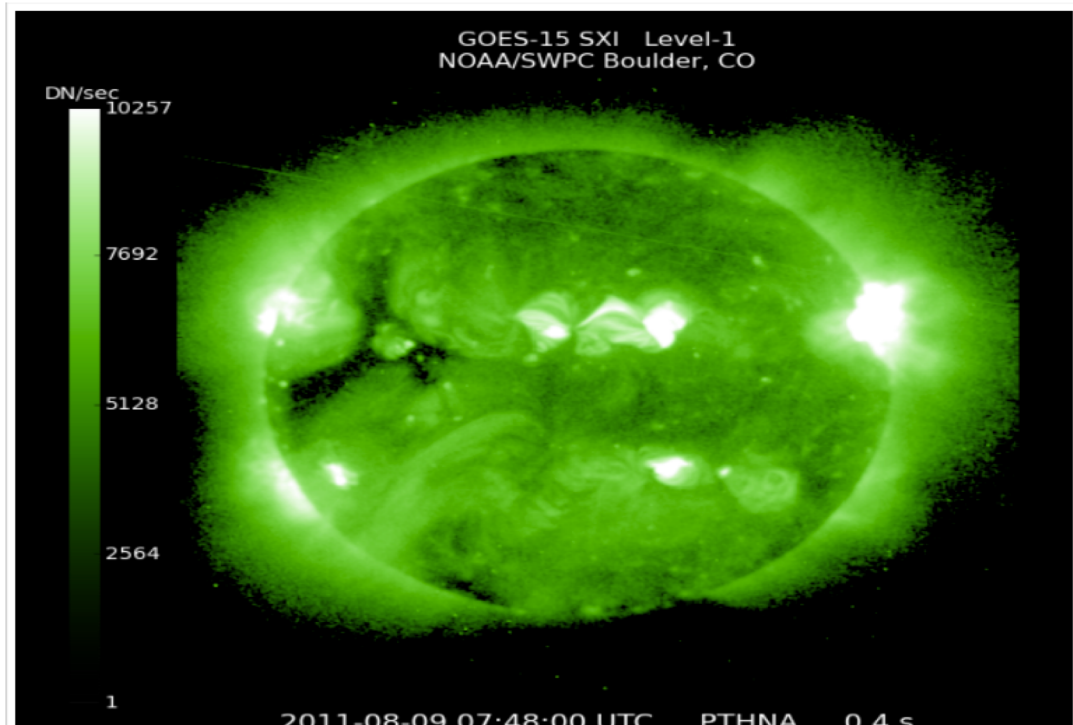
Data

Data from over 500 solar flare events, spanning April 2010 to July 2017, including GOES C-, M-, and X-class solar flares at various intensities, were collected from the Space Weather Database Of Notifications, Knowledge, Information (DONKI) developed at the NASA Goddard Space Flight Center (GSFC) Community Coordinated Modeling Center (CCMC). Historical GOES satellite (NOAA) X-ray flux (NASA GSFC CCMC integrated Space Weather Analysis system (iSWA)) time series data are available for all solar flare events of the sample set. The GNSS daily observation data, archived at the NASA GSFC Crustal Dynamics Data Information System (CDDIS), are used to probe F-region reactions to increased ionization, complementing GOES space-based X-ray observations. CDDIS provides GNSS data with continuous 24-hour coverage from multiple satellites, at a temporal resolution of 30 seconds from over 400 stations.

Poster Summary

For this poster we present a case study of one, strong solar flare event - the X6.9 class solar flare that occurred August 9, 2011 around 08:05 UTC (Figure 2). CDDIS data with continuous coverage from 100 unique GNSS receiver stations, spanning 20 countries at a variety of geographic locations, are extracted and analyzed for signatures indicating flare detection. The geographic distribution of receivers enables us to explore the effects of this solar flare intensity at localized regions in Earth's ionosphere around the globe. The GNSS observations are combined with GOES data to characterize the multi-frequency signatures found, and to explore the impact of this strong solar flare event through the upper and lower layers of the Earth's ionosphere.

GOES X-ray (Space)



X6.9 class solar flare
Start time: 07:48 UTC
Peak time: 08:05 UTC
End time: 08:08 UTC
Source location: N17W69
Active region number: 11263

Figure 2: GOES-15 Solar X-ray Imager (SXI) capturing the active Sun at the event start time; the heat bar displays the data number (DN or discretized charge per pixel) per second (NOAA SWPC Boulder, CO; courtesy of NASA iSWA)

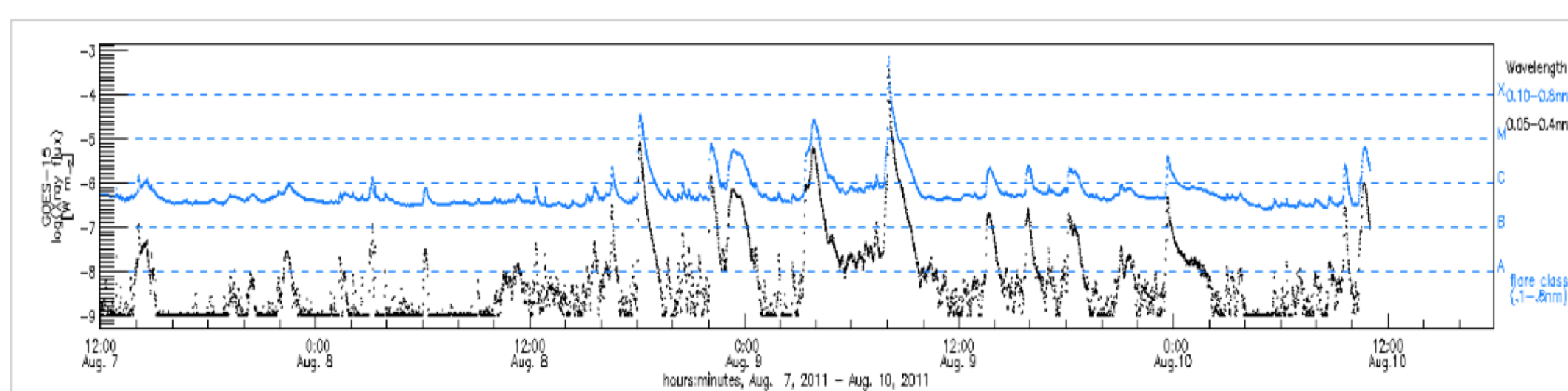
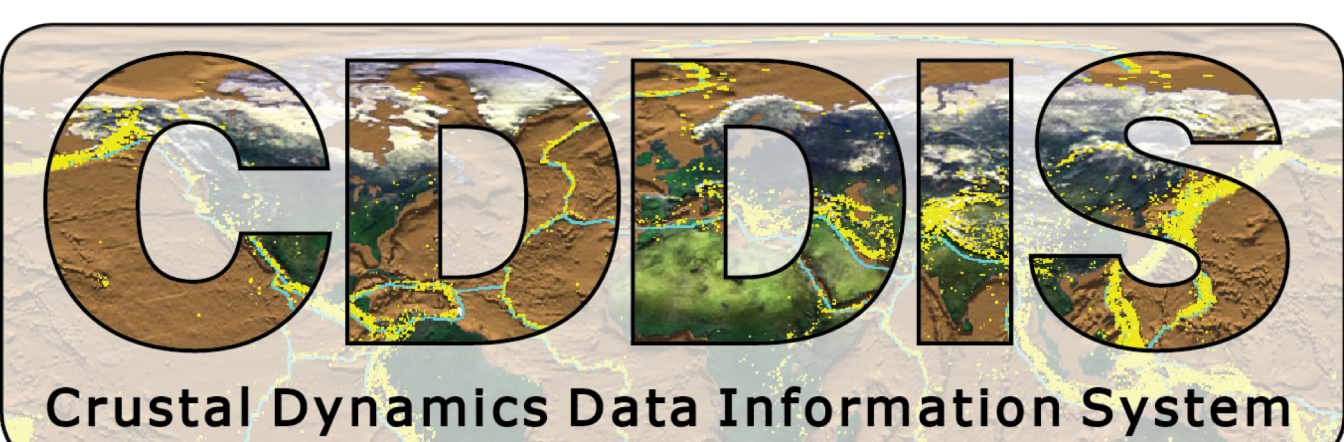


Figure 3: GOES-15 x-ray flux over the time of the solar flare event shown in black (wavelength range = 0.05 - 0.4 nm) and blue (wavelength range = 0.1 - 0.8 nm); the dashed horizontal lines measure flare class (plot from CCMC iSWA)



<https://cddis.nasa.gov>

GNSS (F-region)

A GNSS data extraction script, written in Python, was developed at the CDDIS to read RINEX version 2.11 o-files and extract observations, reported every 30 seconds, spanning 24 hours per each GNSS satellite with coverage available at the given epoch. Extracted data from 100 unique global GNSS receiver stations were analyzed using dual-frequency carrier phase (L1, L2; full cycles) and pseudorange code (P1, P2; meters) observables to estimate the ionospheric phase advance, group delay, and signal-to-noise ratios for all satellites present in the observations, over all epochs. Figure 4 shows the carrier phase estimates of ionospheric delay for seven stations in different countries. In each subplot a peaky delay feature is present in within this case study's X-class solar flare event time frame (vertical dashed lines). Left-hand subplots in Figure 5 (below) illustrate the delay feature discovered in the LEIJ (Germany) carrier phase observations on the day of the X6.9 class solar flare (August 9, 2011), while the subplots on the right (below) from the same satellite and receiving station, show no signs of the pulse on the day before the event (no documented solar flare events are present in NASA GSFC DONKI on August 8, 2011).

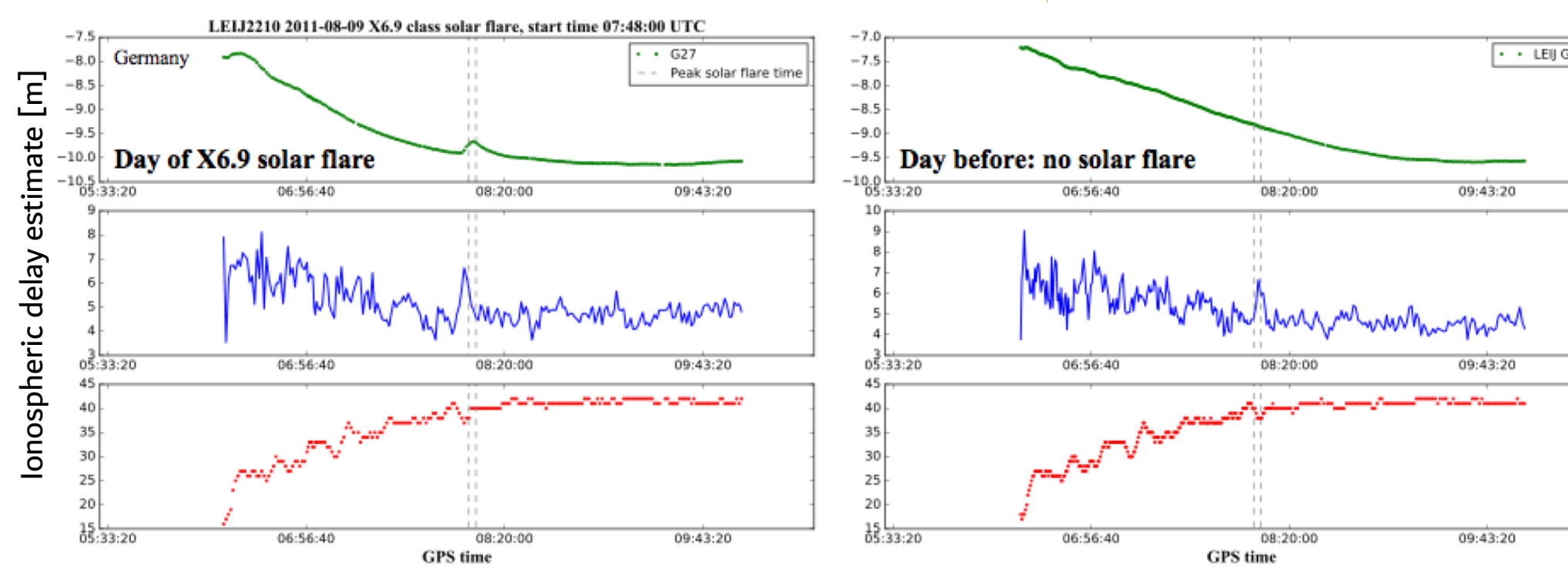


Figure 5: GPS estimates of ionospheric delay plotted with time; the solar flare event is marked by two dashed lines; characteristically smooth carrier phase advance (green) data are plotted on top, followed by noisy pseudorange code delay (blue) in the middle, and receiver-dependent signal-to-noise (red) at the bottom; the total system pseudorange error budget includes the space, control, and user segments with standard deviation values of 7.1 m²

Results

The ionospheric delay "pulse" was discovered in 36% of the case study GNSS observation files (o-files), appearing precisely at the time of the X-class solar flare event, 08:05 - 08:08 UTC. The pulse appears for GPS satellites only; none appear to be present in GLONASS satellite observations. Specific GPS satellites pick up the delay feature, namely satellites G15, G27, G8, and G9, among others. For example, delay features were discovered in 58% of GNSS o-files for G15 satellite observations, specifically. The number of individual satellite observations in o-files with delay features present are found to be higher in specific global regions. Figure 6 shows the number of unique satellites in observation files with a delay pulse present by country.

Conclusion

Figure 7 (right; provided by SWACI*) displays regions of higher TEC densities which indicate higher levels of ionization occurring in the ionosphere at the time of the flare event. GPS signals propagating through these localized regions experience an increased delay due to higher electron densities caused by enhanced x-ray and extreme UV radiation from the solar flare. In Figure 8, GNSS receiving stations with delay features present in observations are plotted as green stars, and stations without pulses are plotted as red circles. This figure illustrates that delay feature occurrences correspond with global regions of higher TEC as compared with Figure 7.

Future work will include expanding the methods presented for this case study to GNSS satellite observations with simultaneous coverage for over 500 solar flare events of different strengths. Metrics such as ionospheric delay, TEC, number of satellites, satellite observing angle, positions, receiving station latitude and longitude, and other practical data can be made available to the community at the CDDIS archive. Your recommendations of useful data and metrics obtained with this study are much appreciated!

Acknowledgements

1 Trinity College Dublin; 2 Space Weather Monitors at Stanford SOLAR Center, Stanford University; 3 *Space Weather Application Center - Ionosphere (SWACI) of the German Aerospace Center e.V. (DLR) in Neustrelitz, Germany; 4 Community Coordinated Modeling Center (CCMC) at NASA GSFC Database Of Notifications, Knowledge, Information (DONKI); 5 Community Coordinated Modeling Center (CCMC) at NASA GSFC iNtegrated Space Weather Analysis tool (iSWA)

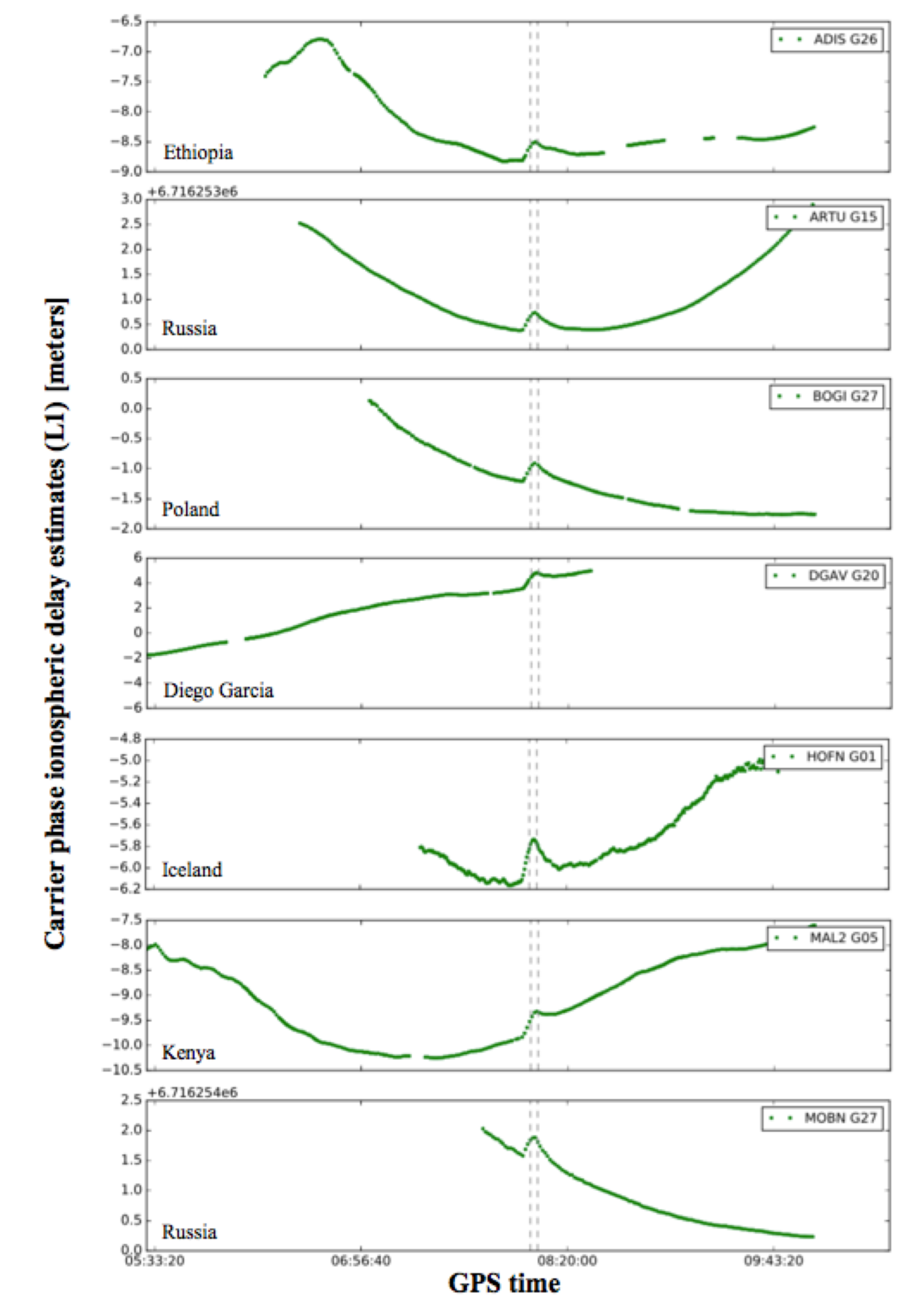


Figure 4: GPS carrier phase estimates of ionospheric delay plotted with time; the solar flare event marked by the two vertical, dashed lines

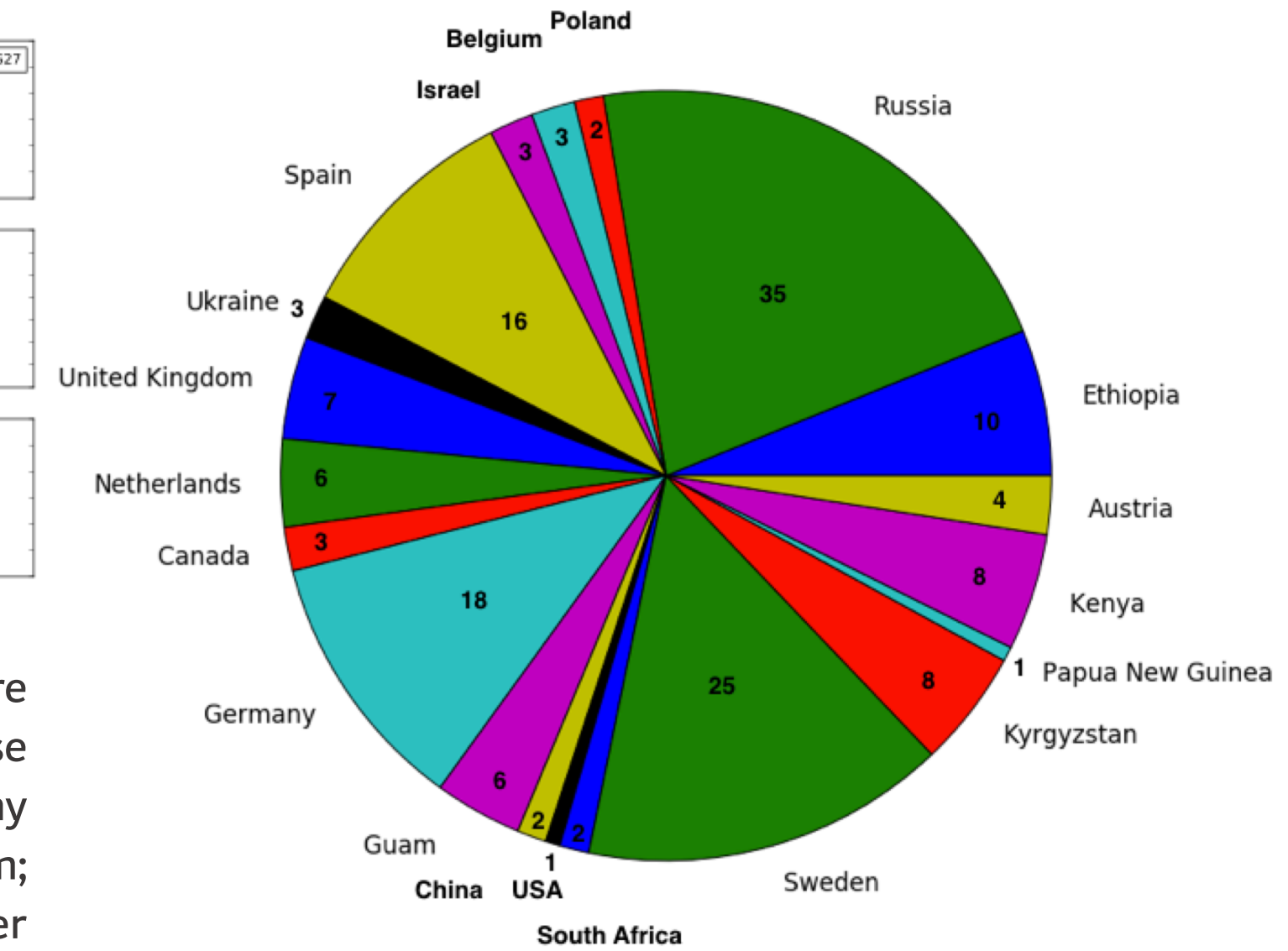


Figure 6: Countries and number of delay features present in unique GPS satellite observations

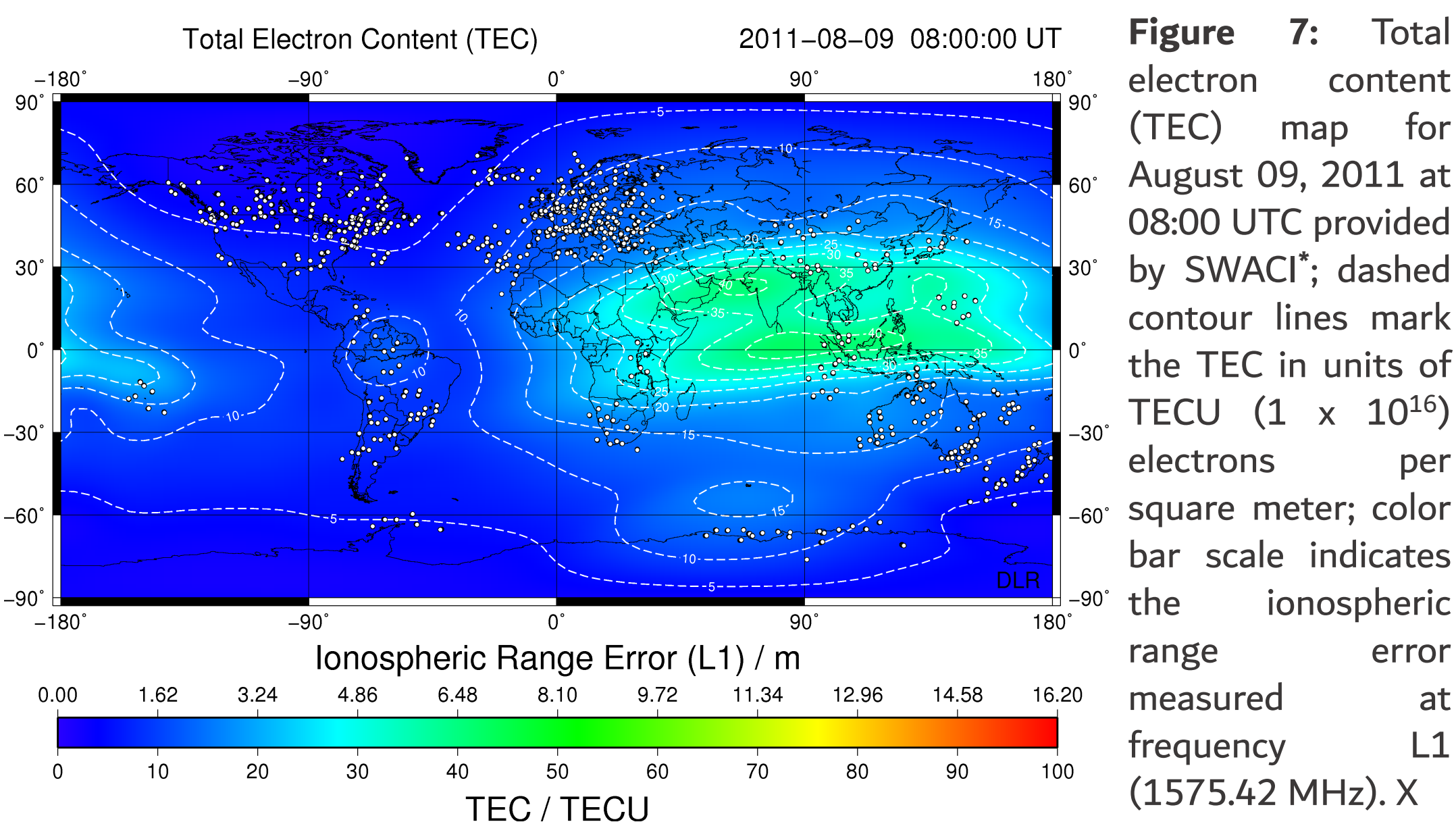


Figure 7: Total electron content (TEC) map for August 09, 2011 at 08:00 UTC provided by SWACI*; dashed contour lines mark the TEC in units of TECU (1×10^{16} electrons per square meter); color bar scale indicates the ionospheric range error measured at frequency L1 (1575.42 MHz). X

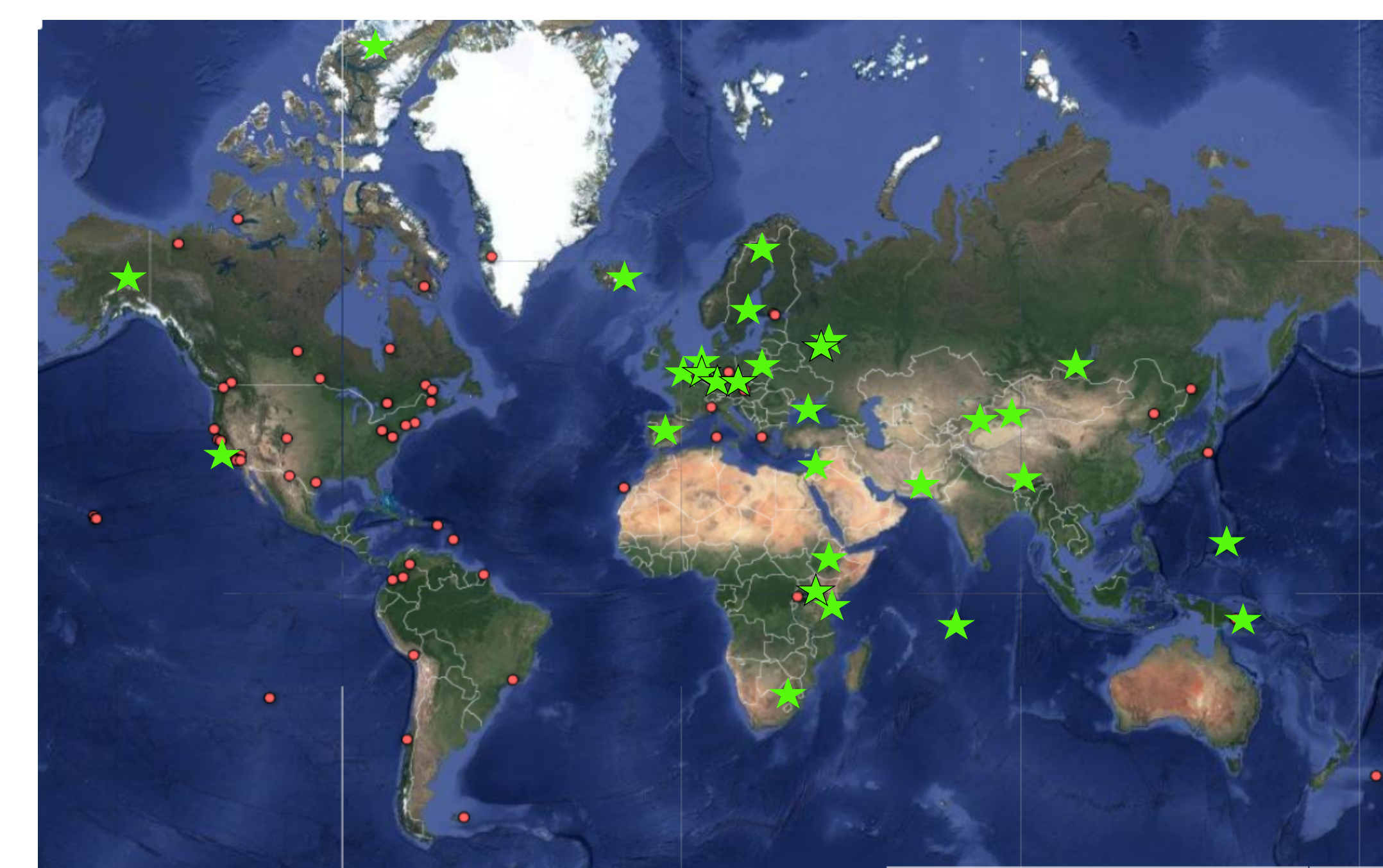


Figure 8: World map with red circles marking GNSS receiver stations with NO pulse present in observations, and green stars marking those WITH a delay pulse present

